TECHNICAL REPORT

Defense Threat Reduction Agency
8725 John J. Kingman Road, MS
6201 Fort Belvoir, VA 22060-6201

DTRA-TR-15-63

Penetration into Granular Earth Materials (Topic H): A Multi-scale Physics-Based Approach Towards Developing a Greater Understanding of Dynamically Loaded Heterogeneous Systems

Distribution Statement A. Approved for public release, distribution is unlimited.

August 2016

HDTRA1-09-1-0045

John Borg

Prepared by:
Marquette University
1324 West Wisconsin Avenue
Milwaukee, WI 53233

DESTRUCTION NOTICE:

Destroy this report when it is no longer needed.
Do not return to sender.

PLEASE NOTIFY THE DEFENSE THREAT REDUCTION AGENCY, ATTN: DTRIAC/ J9STT, 8725 JOHN J. KINGMAN ROAD, MS-6201, FT BELVOIR, VA 22060-6201, IF YOUR ADDRESS IS INCORRECT, IF YOU WISH IT DELETED FROM THE DISTRIBUTION LIST, OR IF THE ADDRESSEE IS NO LONGER EMPLOYED BY YOUR ORGANIZATION.

REPORT DOCUMENTATION PAGE	*Form Approved* *OMB No. 0704-0188*

1. REPORT DATE *(DD-MM-YY)*
00-09-16

2. REPORT TYPE
Technical

3. DATES COVERE-D *(From - To)*
01 July 2009 – 31 April 2015

4. TITLE AND SUBTITLE
PENETRATION INTO GRANULAR EARTH MATERIALS (TOPIC H): A MULTI-SCALE PHYSICS-BASED APPROACH TOWARDS DEVELOPING A GREATER UNDERSTANDING OF DYNAMICALLY LOADED HETEROGENEOUS SYSTEMS

5a. CONTRACT NUMBER
HDTRA1-09-1-0045

5b. GRANT NUMBER

5c. PROGRAM ELEMENT NUMBER

6. AUTHOR(S)
John Borg

5d. PROJECT NUMBER

5e. TASK NUMBER

5f. WORK UNIT NUMBER

7. PERFORMING ORGANIZATION NAME(S) AND ADDRESS(ES)
Marquette University
Office of Research and Sponsored Programs Holthusen Hall, 341
1324 West Wisconsin Avenue
Milwaukee, WI 53233

8. PERFORMING ORGANIZATION REPORT NUMBER

9. SPONSORING/MONITORING AGENCY NAME(S) AND ADDRESS(ES)
Defense Threat Reduction Agency
8725 John J. Kingman Rd
Fort Belvoir, VA 22060-6201

10. SPONSORING/MONITORING AGENCY ACRONYM(S)
DTRA

11. SPONSORING/MONITORING AGENCY REPORT NUMBER(S)
DTRA-TR-15-63

12. DISTRIBUTION/AVAILABILITY STATEMENT
Distribution Statement A. Approved for public release, distribution is unlimited.

13. SUPPLEMENTARY NOTES

14. ABSTRACT

15. SUBJECT TERMS Sand, Heterogeneous, impact velocities, granular

16. SECURITY CLASSIFICATION OF: a. REPORT	b. ABSTRACT	c. THIS PAGE	17. LIMITATION OF ABSTRACT:	18. NUMBER OF PAGES	19a. NAME OF RESPONSIBLE PERSON (Monitor)
U	U	U	SAR	19	Su Peiris **19b. TELEPHONE NUMBER** *(Include Area Code)* (703) 767-4732

Standard Form 298 (Rev. 8-98)
Prescribed by ANSI Std. Z39-18

UNIT CONVERSION TABLE

U.S. customary units to and from international units of measurement*

U.S. Customary Units	Multiply by → ← Divide by†		International Units
Length/Area/Volume			
inch (in)	2.54	$\times 10^{-2}$	meter (m)
foot (ft)	3.048	$\times 10^{-1}$	meter (m)
yard (yd)	9.144	$\times 10^{-1}$	meter (m)
mile (mi, international)	1.609 344	$\times 10^{3}$	meter (m)
mile (nmi, nautical, U.S.)	1.852	$\times 10^{3}$	meter (m)
barn (b)	1	$\times 10^{-28}$	square meter (m^2)
gallon (gal, U.S. liquid)	3.785 412	$\times 10^{-3}$	cubic meter (m^3)
cubic foot (ft^3)	2.831 685	$\times 10^{-2}$	cubic meter (m^3)
Mass/Density			
pound (lb)	4.535 924	$\times 10^{-1}$	kilogram (kg)
unified atomic mass unit (amu)	1.660 539	$\times 10^{-27}$	kilogram (kg)
pound-mass per cubic foot (lb ft^{-3})	1.601 846	$\times 10^{1}$	kilogram per cubic meter (kg m^{-3})
pound-force (lbf avoirdupois)	4.448 222		newton (N)
Energy/Work/Power			
electron volt (eV)	1.602 177	$\times 10^{-19}$	joule (J)
erg	1	$\times 10^{-7}$	joule (J)
kiloton (kt) (TNT equivalent)	4.184	$\times 10^{12}$	joule (J)
British thermal unit (Btu) (thermochemical)	1.054 350	$\times 10^{3}$	joule (J)
foot-pound-force (ft lbf)	1.355 818		joule (J)
calorie (cal) (thermochemical)	4.184		joule (J)
Pressure			
atmosphere (atm)	1.013 250	$\times 10^{5}$	pascal (Pa)
pound force per square inch (psi)	6.984 757	$\times 10^{3}$	pascal (Pa)
Temperature			
degree Fahrenheit (°F)	$[T(^{o}F) - 32]/1.8$		degree Celsius (°C)
degree Fahrenheit (°F)	$[T(^{o}F) + 459.67]/1.8$		kelvin (K)
Radiation			
curie (Ci) [activity of radionuclides]	3.7	$\times 10^{10}$	per second (s^{-1}) [becquerel (Bq)]
roentgen (R) [air exposure]	2.579 760	$\times 10^{-4}$	coulomb per kilogram (C kg^{-1})
rad [absorbed dose]	1	$\times 10^{-2}$	joule per kilogram (J kg^{-1}) [gray (Gy)]
rem [equivalent and effective dose]	1	$\times 10^{-2}$	joule per kilogram (J kg^{-1}) [sievert (Sv)]

*Specific details regarding the implementation of SI units may be viewed at http://www.bipm.org/en/si/.
†Multiply the U.S. customary unit by the factor to get the international unit. Divide the international unit by the factor to get the U.S. customary unit.

Final Report
HDTRA1-09-1-0045

May 20, 2015

Prepared by John Borg (PI), Dept. Mechanical Engineering, Marquette University
1515 W. Wisconsin Street, Milwaukee Wisconsin,
(414) 288-7519 ***john.borg@mu.edu***

Grant/Award #: HDTRA1-09-1-0045
PI Name: John Borg
Organization/Institution: Marquette University
Project Title: Penetration into Granular Earth Materials (Topic H): A Multi-scale Physics-Based Approach Towards Developing a Greater Understanding of Dynamically Loaded Heterogeneous Systems

TABLE OF CONTENTS

1. SUMMARY 5

WHAT ARE THE MAJOR GOALS OF THE PROJECT? 5
WHAT OPPORTUNITIES FOR TRAINING AND PROFESSIONAL DEVELOPMENT HAS THE PROJECT PROVIDED? 6
HOW HAVE THE RESULTS BEEN DISSEMINATED TO COMMUNITIES OF INTEREST? 7
WHAT WAS ACCOMPLISHED UNDER THESE GOALS? 7

2. EXPERIMENTATION 7

2.1. DYNAMIC DART GUN EXPERIMENTS: 8
2.2. QUASI-STATIC COMPRESSION EXPERIMENTS: CHARACTERIZING DAMAGED SAND 11
2.3. ULTRA-SONIC PULSE-RECEIVER TESTS: ELASTIC WAVE CHARACTERIZATION OF WET AND DRY SAND 12
2.4. PHOTON DOPPLER VELOCIMETRY (PDV) 13

3. COMPUTATIONAL SIMULATIONS 14

3.1. Mesoscale Simulations 14
3.2. CONTINUUM SIMULATIONS 15

4. DISCUSSION 16

5. REFERENCES 16

1. Summary

New experimental techniques have been developed to aid understanding of impact, penetration, and cavity formation associated with high-speed projectile penetration of sand. A new half-inch gun was constructed for this project. A "quarter-space" target geometry is used with a transparent window, coupled with high-speed photography and digital image correlation (DIC or PIV). These techniques are able to capture the bulk-to-grain response at impact velocities in a range from 30 to 350 m/s. Results indicate formation of stress bridges, dynamic grain damage, and fracture. The transmitted stress waves were captured using a quartz load cell, the results from which were compared to DIV measurements and simulations. The load cell provides high temporal resolutions however it averages over a large region (the face of the gage). The PIV technique provides information at the grain scale but suffers from low temporal resolution.

Experiments were conducted at Marquette University (MU) and the Naval Surface Warfare Center (NSWC) in Indian Head Maryland. Dr. Borg and his students travelled to NSWC and brought the half-inch gun with them. Data was collected utilizing NSWC's Cordin 550, 64 frame, high-speed camera. In addition, several student participated in the *Naval Research Internship Program*. The experience of establishing a working collaboration between the University and the DoD was a valuable opportunity for students, faculty and members of staff alike.

Simulations were performed to supplement experiments and utilize both a mesoscale and continuum approach. The mesoscale simulations resolve grain-on-grain interactions and do not require additional constitutive relations. The continuum approach is useful for system level simulations. The question we want to probe is what mechanical mechanisms must be included in the mesoscale and continuum simulations in order to realize the experimentally observed penetration behavior. The simulations capture the early time stress wave history, crater formation and stress bridging phenomena. However, the late time results are not well resolved.

The final aspect of this work is to build and deploy a Photon Doppler Velocimetry (PDV) system. This system will make it possible to explore a wider range of granular phenomena because all the data within the laser spot can be temporally resolved. This would allow for the distributions of particle velocities to be measured. The MU-PDV has been built and tested on solid materials where the response is better understood. Measurements on granular materials are forthcoming.

This report outlines work completed thus far from Grant HDTRA-09-1-0045. This work is in support of the Basic and Applied Sciences Directorate and the JSTO and Penetration of Granular Earth Materials: A Multi-scale Physics-Based Approach Towards Developing a Greater Understanding of Dynamically Loaded Heterogeneous Systems.

What are the major goals of the project?

The major goals of this project are:

1. directly observe and measure the complex projectile-target interactions in order develop a better understanding of the penetration dynamics,
2. explore the use of mesoscale computational techniques to gain better understanding of important phenomenology (grain-on-grain interactions, dynamic force chains, etc.) associated with the penetration of earth materials,
3. formulate new analytic methods to describe and quantify penetration dynamics,
4. introduce and educate the next generation of STEM workers with a skill set applicable to conduct basic research in and solve complex problems for defense-related areas,
5. build the knowledge base of penetration dynamics so that designers can predict and control penetration performance (including projectile stability and depth) in earth materials to ultimately meet operational objectives.
6. develop ultrasonic techniques to probe bulk density characteristics,
7. perform mesoscale simulations focusing on strain-to-failure criteria,
8. investigate hydrodynamic pressure effects in the target system,
9. develop and deploy a Photon Doppler Velocimetry techniques for *in situ* stress distribution measurements,
10. increase launch velocity clearly above elastic sound speed.

What opportunities for training and professional development has the project provided?

Education: Six graduate students and five undergraduate students were supported by this grant. To date 5 of the graduate students have graduated and one is currently working towards graduation, expected May 2016. Two of the graduate students when on to work for DoD and one for DoE: Kenneth Jordan (NSWC-Dahlgren) and Andrew Fraser (DoD-Cold Regions Research and Engineering Laboratory) and Cheryl Perich. Three of the undergraduates have gone onto graduate school; Cheryl Perich completed her Master's degree at Cornell University, Jeff Midday completed a Master's degree at the University of Nebraska, and Nathaniel Helminiak will start a Master's program at Marquette University in June 2015.

Students Supported Under this Project:

Graduate Student	**Degree**	**Starting**	**Finishing**	**Support**
1. Peter Sable	MSME	May 2014	Expected 2016	DTRA Full Support
2. Andrew Van Voreen	MSME	May 2011	Graduated 2013	DTRA Full Support
3. Cullen Braun	MSME	Sept. 2009	Graduated 2011	DTRA and MU Teaching Assistant
4. Ken Jordan[1]	PhD - ME	Sept. 2006	Graduated 2011	DTRA and Navy SMART Fellow
5. Drew Fraser	MSME	Jan 2007	Graduated 2010	DTRA Full Support
6. Michael Morrissey	MSME	Sept. 2007	Graduated 2009	DTRA and MU Teaching Assistant
Undergraduate Student				
1. Trent Wolff	BSME (2017)	May 2013	July 2013	DTRA Summer Student
2. Nathaniel Helminiak	BSME (2016)	May 2013	July 2013	DTRA Summer Student
3. Jonathan Sobeck	BSME (2013)	May 2011	July 2011	DTRA Summer Student
4. Jeff Midday	BSME (2010)	May 2010	July 2010	DTRA Summer Student
5. Cheryl Perich[2]	BSME (2009)	May 2009	July 2009	DTRA Summer Student

1. Currently Employed at Naval Surface Warfare Center, G-Division
2. Currently Employed at Sandia National Laboratories

Conferences: This work has provided opportunities for several students to present their work in public forums such as conferences and workshops. These kinds of activities help connect the student to the field at large and help guide research progress by developing dialog and feedback from peers. Peter Sable presented at the Society for Experimental Mechanics Graduate student Conference at the University of Wisconsin in March 2015 and will present at the up-coming APS-SCCM conference in Tampa Fl. Andrew Van Vooren presented at the Hyper Velocity Impact Symposium (HVIS) in 2012 (Baltimore) and the SEM in 2013 (Chicago). Ken Jordan presented his results and Andrew Fraser, along with an undergraduate co-author Jonathan Sobeck, both presented at the APS-SCCM conference in Chicago in 2011. See the next section for references.

How have the results been disseminated to communities of interest?

The results have been disseminated through peer review journals and conference presentations and proceedings In addition, several PIs funded from this topical area, under the leadership of Magued Iskander at NYU Polytechnic School, wrote a book to be published by Elsevier Press. The book will ship in July 2015. The following is a complete list of publications which have been written based on this work:

1. J.P. Borg, J.P., Van Vooren, A. and Morrissey, M. In Situ Characterization Of Projectile Penetration Into Sand, *Chapter 6* in *Rapid Penetration into Granular Media* by Magued Iskander, **Elsevier Press**, 38 page manuscript, July 2015
2. Borg, J.P., Morrissey, M. Perich, C. Vogler, TJ and Chhabildas, L. *In Situ Velocity and Stress Characterization of a Projectile Penetrating a Sand Target: Experimental Measurements and Continuum Simulations*. **Inter. J. of Impact Eng** 51, 2013, pg. 23-35
3. Borg, J. Van Vooren, A., Sandusky' H. and Felts, J., Sand Penetration: A Near Nose Investigation of a Sand Penetration Event, Dynamic Behavior of Materials, Volume 1 **Proceedings of the 2013 Annual Conference on Experimental and Applied Mechanics**, Song, Bo; Casem, Dan; Kimberley, Jamie (Eds.) p. 452. Chicago, 2013
4. Van Vooren, A., Borg, J., Sandusky, H. and Felts, J., Sand Penetration: A Near Nose Investigation of a Sand Penetration Event, ***Proceedings of the 11th Hypervelocity Impact Symposium***, Procedia Engineering, Volume 58, 2013, Pages 601–607.
5. Jordan, K. and Borg, J.P. Resolving the Shock Wave Profile in Viscous Fluids. **Proceedings from 17th APS-SCCM-Shock Compression of Condensed Matter – 2011,** M. L. Elert, W. T. Buttler, J. P. Borg, J. L. Jordan, and T. J. Vogler, eds., AIP Conference Proceedings vol. 1426, New York, 2012
6. Borg, J.P., Braun, C. Fraser, A., Sobeck, J. and Van Vooren, A. Ballistic Penetration of Sand With Small Caliber Projectiles. **Proceedings from 17th APS-SCCM-Shock Compression of Condensed Matter – 2011,** Elert, Buttler, J. Borg, J. Jordan, and T. Vogler, eds., AIP Conference Proceedings vol. 1426, New York, 2012

What was accomplished under these goals?

The following summarizes the experiments and simulations carried out in this work.

2. Experimentation

The experimental techniques include observing semi-infinite targets (meaning targets where one side is made of an optically accessible transparent material) and launching projectiles along the side of the view window to observe the projectile/target interaction. Within the current effort, we want to narrow the field of view of these experiments in order to observe and resolve the grain-on-grain interactions, including the removal of porosity, the formation of a bow shock, the formation of dynamic stress bridging, grain facture and excavation. We are specifically interested in the area near the nose of the projectile where high stress states are achieved. These experiments are being conducted on a relatively small scale (5 mm diameter projectiles) in order to simplify the analysis. Experiments at and below 100 m/s have been completed. We are currently reconfiguring the gun in order to achieve speeds in the range of 30 to 350 m/s. Experiments have been conducted at both Marquette University and the Naval Surface Warfare Center in Indian Head, Maryland. Students have worked at both facilities and have participated in the ***Naval Research Internship Program*** during the course of the grant period.

2.1. Dynamic Dart Gun Experiments:

Figure 1 presents the gun launcher and target tank. This entire setup was constructed at Marquette during the grant period in order to facilitate the objectives of the grant. The launcher is currently capable of launching 4 inch long, 0.25 inch diameter, aluminum projectiles at just over 100 m/s. Figure 1 also presents the target tank with quartz gages installed. From high-speed images it is possible to discern grain-on-grain interactions. This launcher has twice been moved to Indian Head in order to perform experiments while utilizing the Cordin 550 high speed camera.

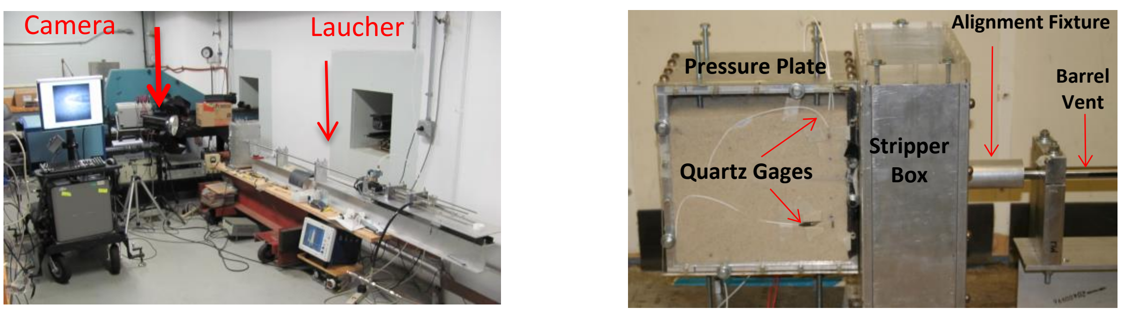

Figure 1. Layout of the experimental apparatus including the target tank**.**

Table 1 presents the combinations of experimental configurations. In this table green represents the combination experimental parameters completed, red represents the combinations not yet explored, and grey represents combination that are not possible. Given space limitations, a full report of the experimental results will not be presented here.

Table 1. Tests Completed Matrix

	High Confine Pressure	Low Confine Pressure	Velocity Range	Cone	Flat	Hemi	Zoomed Out	Zoomed Mid	Zoomed In	Entrance View
High Pressure										

Low Pressure										
Velocity Range										
Cone										
Flat										
Hemi										
Zoomed Out										
Zoomed Mid										
Zoomed In										
Sand Entrance View										

Figure 2 a 40 m/s shots along with the post-processed a Particle Image Velocimetry (PIV) image. These images indicate that a cavity has formed around the projectile and that there is little contact between the sand and projectile along the length of the projectile. Most of the projectile-sand interaction is confined to the nose of the projectile. In addition to the optical measurements, stress profiles in the sand were measured using a load cell, the location of which is indicated in red in Fig. 2a. Figure 3 presents a comparison of the PIV and load cell data.

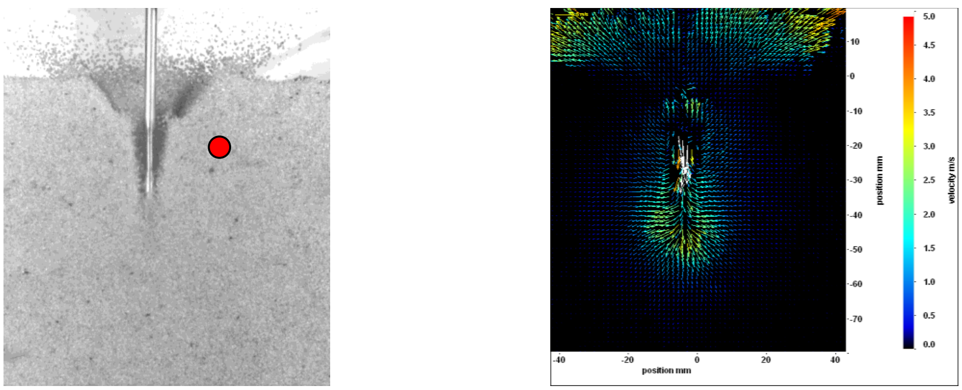

a) High-speed photography

b) Post-processed image of (a)

Figure 2. High-speed light photography of a long rod projectile impacting a semi-infinite sand target at 40 m/s. b) PIV convolution of real-time stress field. Time accurate velocity data collected at red marker in a) is presented in Fig 3.

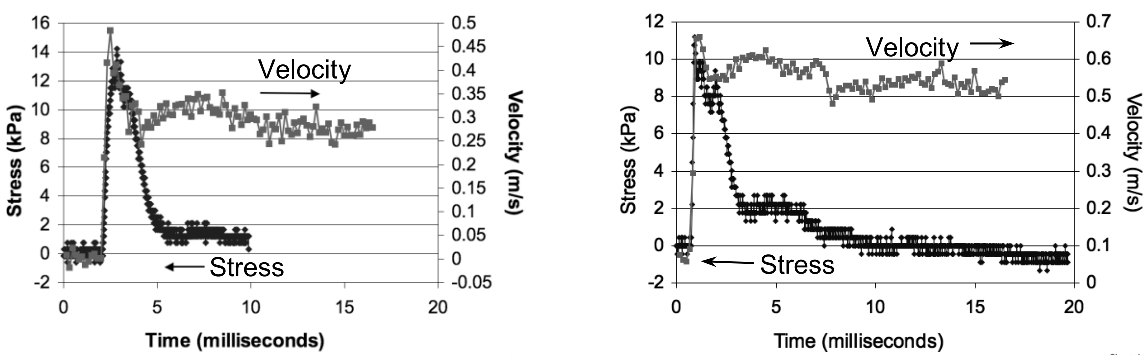

(a) Flat Nose Right Cylinder Projectile – 35 m/s

(b) Spherical Projectile – 128 m/s

Figure 3. Velocity and stress measurements at a fixed marker in the sand located 5 mm from the shot-line and 20 mm below the free surface, approximately indicated by the red marker in Fig. 1.

As the launch velocity is increased to near 100 m/s a two-wave structure is observed in the sand: a separated bow shock (or compression wave) and a damage wave, which remains near the leading edge of the dart. The bow shock, which has been observed by others, travels at roughly 100 m/s. However, a new discovery in this work is the presence of the damage wave, which is presented in Figure 4. This wave is essentially a wispy bright region near the nose of the dart, which travels along with the dart. When first observed, it was not clear as to why these grains appear brighter, i.e. whiter, than their neighboring grains. We speculate that the reason the grains appear white is because of an increase in light reflectance as compared to neighboring grains. Since the camera and the lighting are on the same side of the target, an increase in reflectance of a grain would result in more collected light by the camera, and would therefore appear brighter. In order to explore this further a series of quasi-static tests were carried out and will be reviewed in the following section.

Figure 5 presents a series of extreme close-up high-speed images, where individual grains can be discerned, recorded directly in front of the projectile along the shot line. These imagies were obtained at NSWC-IH using the Cordin 550 high speed camera. The projectile, which is not in the field of view, is moving from right to left. It is interesting to note the grain rearrangement and damage during compaction damage. The circle in frame 5a highlights a specific grain, which by the final frame appears to have fractured. Since this field of view is in front of the projectile, we observe grain fracture, before the projectile arrives, under ostensibly normal compressive load. Notice the points of bright light that emanate from this grain before fracture occurs. ***These imagines illustrate, for the first time, a direct observation of the grain dynamics during a high-speed penetration event.*** These imagines and the dynamics we observe will prove invaluable in our assessment of computational schemes presented in the following section.

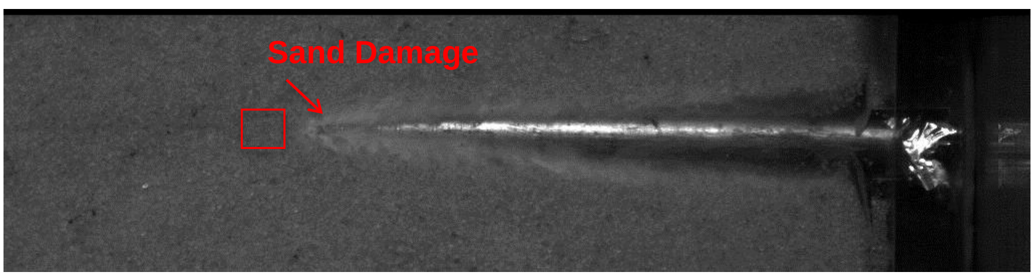

Figure 4: Penetration at approximately 100 m/s. Regions in white near the nose of the projectile represent damaged sand. Enlarged view of box is presented in Figure 5.

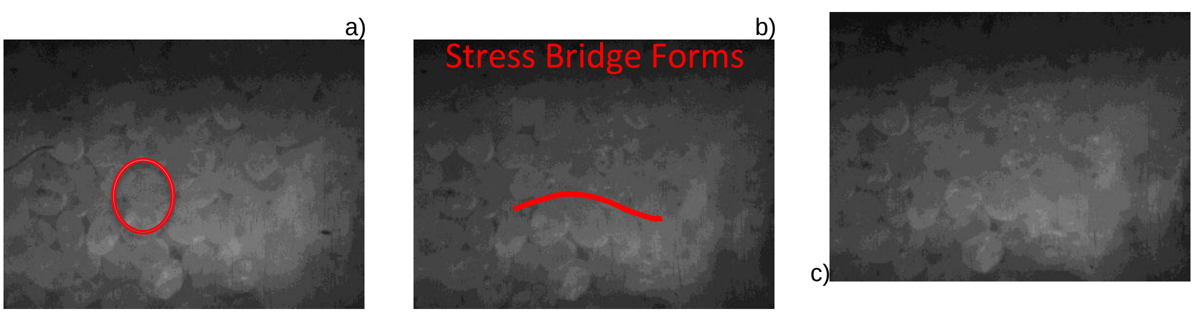

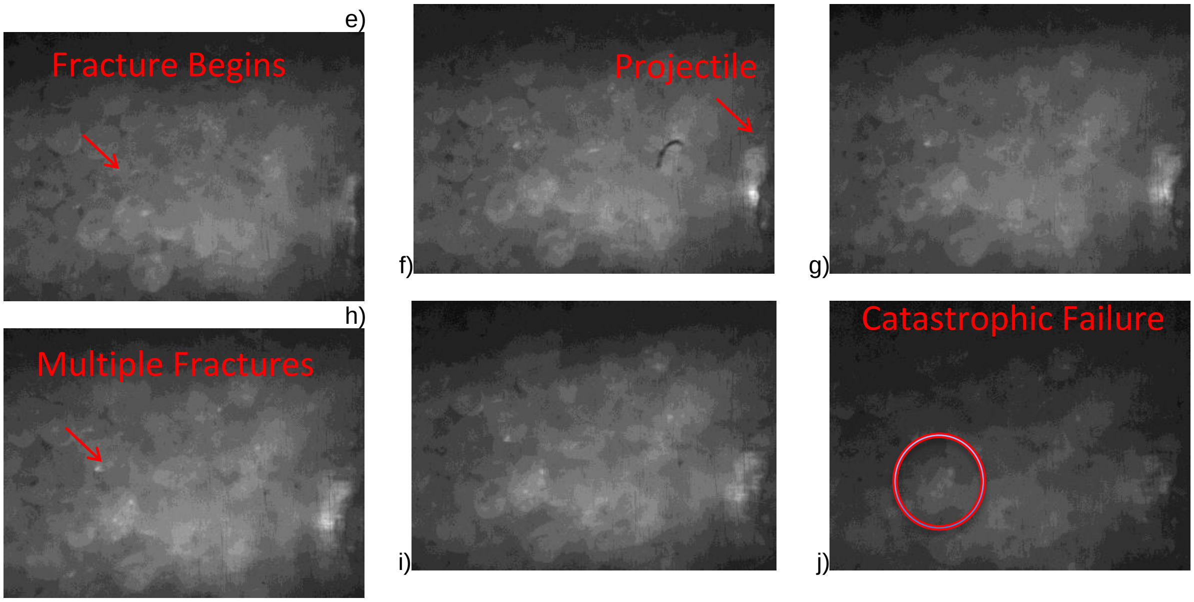

Figure 5. Enlarged view of sand impacted with projectile traveling initially at from right to left. New bright spots within grains indicated new fractured surfaces reflecting light. The grain indicated in frame a) is involved in the formation of a 5 grain stress bridge. The grain begins to fracture in frame e) and catastrophically fails by frame i)

2.2. Quasi-static Compression Experiments: Characterizing Damaged Sand

In order to address the increase in light collected near the nose of the projectile, we performed a set of canonical experiments in which individual grains were damaged in a quasi-static configuration, in a configuration similar to the dynamics experiments. In these experiments, single grains of sand were placed between two metal plates, equipped with a force transducer. Pressure was slowly increased on the grain by moving the plates together until the grain began to fracture, cleave and eventually completely crush. Over numerous trials, it was observed that new crack formations locally increase reflectivity. This process was filmed with a high-speed camera and a 5X lens. This process is inherently random given that only fracture surfaces aligned such that they reflect light back to the camera appear illuminated. Figures 6 and 7 present a typical frame before and after a crack face has formed (1 thousandth of a second apart); this process provides an explanation of the wispy white regions observed in Fig. 4, and the formation of bright spots in Fig. 5. In order to make certain that this phenomenon was not a result of self-luminescence this experiment was repeated in low light conditions; however no light was observed.

In an attempt to measure a stress-strain relation, the initial grain height and the grain height from the frame before fractured occurred were recorded; the ratio of these two heights was recorded as the strain at fracture. Simultaneously, the force on the transducer, divided by the initial height of the grain squared, was recorded as the stress. This was then repeated for the last fracture before the grain was completely crushed. These two data points were recorded as the first and second fractures respectively. This was repeated and the results are presented in Figure 7, which is an analog to a stress-strain relation for a randomly oriented grains. This data suffers from not knowing the area over which the force is applied, or the effect of grain pre-damage and crystallographic orientation with respect to the loading direction. However, it does provide an estimate of the fracture strength of the grains.

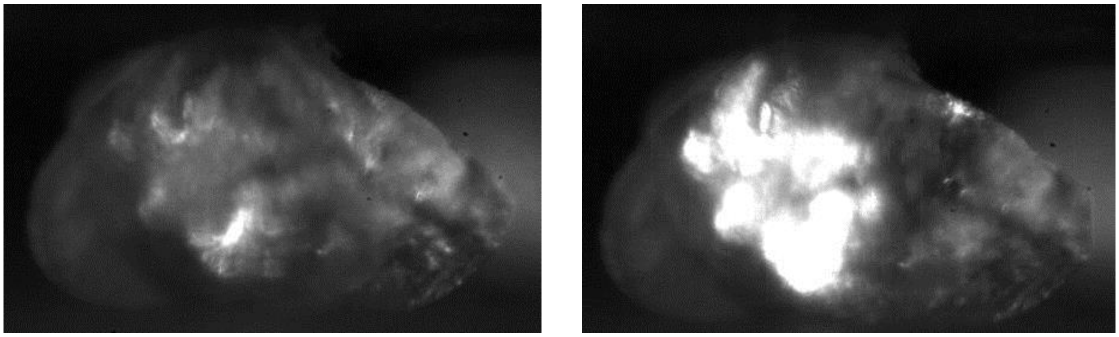

a) Unloaded sand grain b) loaded grain illustrating higher reflectance due to damage

Figure 6. A single grain of sand before and after the crack face has formed. We observe that the presence of the crack results in greater reflectivity and thus more light collected.

In general a straight line can be fit through the majority of the data, with several outliers. The low stress high strain outlier data most likely results when the top portion of the grain completely fractures off before the final fracture has occurred; this would give an unreasonably high value for the “strain”. The high stress low strain outlier data could result from crystallographic orientation of the grain. In general, these results may be used to approximate the average strain-to-failure when modeling dart penetration utilizing a peridynamic, strain-to-failure constitutive relation

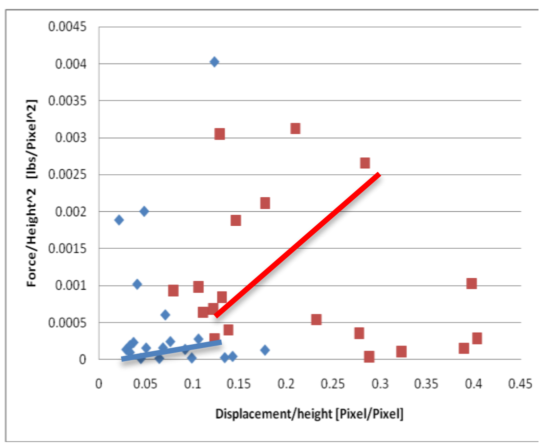

Figure 7. Plot of “stress vs strain” for a single grain of sand

2.3. Ultra-Sonic Pulse-Receiver Tests: Elastic Wave Characterization of Wet and Dry Sand

In order to better characterize the sand the elastic properties of the sand and relate these to the dynamic penetration experiments, ultrasonic pulse-receiver measurements of the sand data were obtained. The objective was to measure the longitudinal and shear elastic wave speeds of a sample of the sand at various static pressures. These measurements could then be compared to the measured wave speeds presented above. This was done to better understand how the various wave speeds effect the penetration curve and fracture.

Figure 8a presents a photograph of the pulse receiver probes. An Olypus 5058PR pulse-reciever unit was used to send and receive pulses; the signals were recorded with high-speed oscillosipte. The results are presented in Figure 8b. The longitudinal and shear wave speeds for sand are presented in Fig. 8b;

the error bars represent the range of values obtained through repeated tests of different sand samples. We interpret the variation in measurements to be a reflection of the variation in sand ensemble arrangements. The average longitudinal speed for dry sand (zero percent water by volume) is near 274 m/s; Liu and Nagle reported averages near 280 m/s [1]. The shock velocity-particle velocity Hugoniot intercept for dry sand was measured in plane strain experiments to be 243 m/s [2]. If we used the group transient time the average longitudinal wave speed would be nearer to 100 m/s. The longitudinal sound speed is reduced when water is added, possibly due to a reduction in grain-on-grain friction which would retard force chain transmissions. The longitudinal sound speed is rather constant over a wide range of moisture contents. As the moisture nears the void volume fraction of sand (28%), the sand becomes completely water saturated. The longitudinal sound speed for saturated sand increases relative to partially saturated sand, but does not recover to longitudinal sound speed of dry sand.

The average shear sound speed of dry sand was measured to be near 208 m/s, with a much larger variation between independent measurements for given grain arrangements, as indicated by the large vertical error bars. With the longitudinal and shear wave speeds we can calculate the elastic properties for dry sand. The average Poisson's ratio was 0.13 but varied from 0 to near 0.15 and the average elastic modulus was 120 MPa and bulk modulus of 36 MPa. The bulk sound speed of sand is 153 m/s, which is far below most shock velocity-particle velocity Hugoniot intercepts for sand [2].

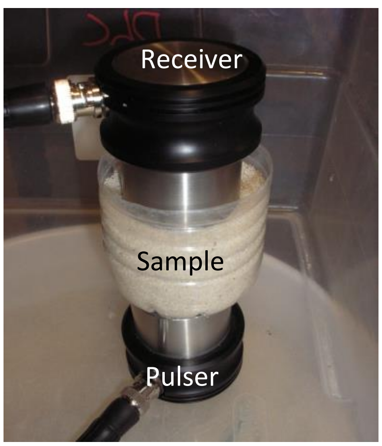

a) Olympus pulse-receiver unit with sand sample

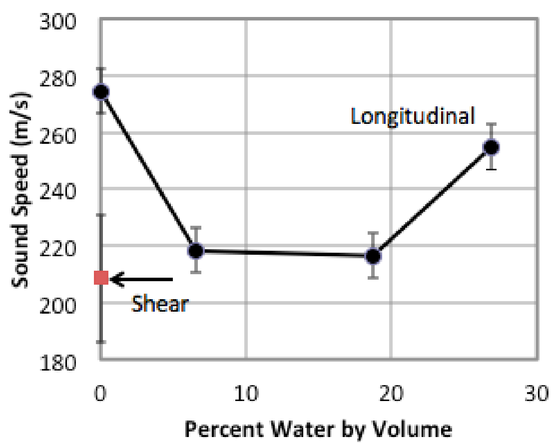

b) Longitudinal and shear sound speed measurements

Figure 8. Pulse-receiver setup and results for longitudinal and shear sound speed measurements.

2.4. Photon Doppler Velocimetry (PDV)

During the final portion of this grant period, the goals included bringing new measurement techniques to bear on the problems being investigated while increasing the overall capabilities at Marquette. In this effort a Photon Doppler Velocimetry (PDV) system was built at Marquette. In order to accomplish this goal the PI attended the PDV Workshop hosted by Sandia National Laboratories in 2012. Dr. Mike Rauls from CalTech was indispensible in getting the MU PDV system up and running. He traveled to Marquette to give a departmental seminar and spent several days building and testing the system. Information gleaned from this experience as well as many helpful suggestions from colleagues, especially Ted Strand and Dan Dolan at Sandia, aided in building a successful system. Figure 9 presents a photograph of the operational system as well as some sample traces obtained while testing the system.

The system has yet to be used to measure the shock profiles generated in granular materials. This will be attempted in the near future.

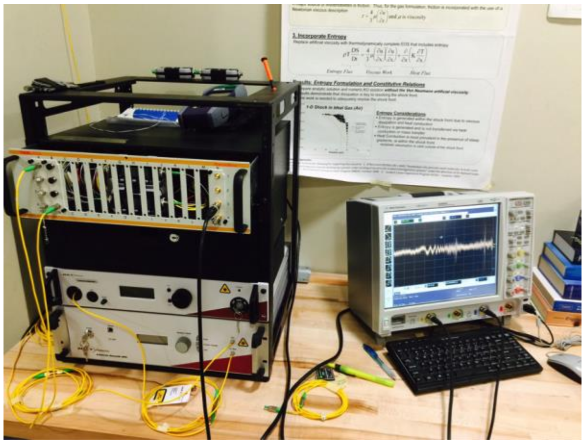

a) Generation 2 Photon Doppler Velocimetry

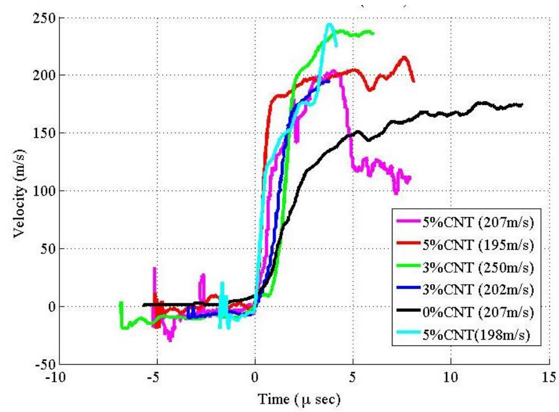

b) Longitudinal and shear sound speed measurements

Figure 9. Photon Doppler Velocimetry (generation 2) setup and results for longitudinal and shear sound speed measurements.

3. Computational Simulations

The computational analysis is two fold. First use mesoscale simulations (continuum, CTH and peridynamic, EMU and LAMPS) to better understand the basic behavior of the heterogeneous system and to develop continuum constitutive relations. Second, to utilize these continuum relations in order to simulate a full-scale continuum impact and penetration event. Mesoscale techniques can be used to augment the near grain-on-grain interaction in ways which are not experimentally accessible. Examples include exploring the projectile behavior as we vary the grain-on-grain friction, the yield or fracture strength. Simultaneously the limitations of computational techniques can be explored. For the continuum analysis several candidate models have been investigated, namely the P-alpha and P-lambda compaction models.

3.1. Mesoscale Simulations

We have been simulating the impact and penetration experiments described above over a range of impact velocity from 40 m/s to 200 m/. The results of which are presented in Figures 9 and 10 respectively, where Figure 8 presents an experimentally obtained image for comparison. The two-wave behavior observed experimentally, i.e. the compaction and damage waves, is indicated in the simulations in red and blue respectively. ***These images are the first (known by the author) that observe a distinct compaction and damage wave ahead of the projectile.***

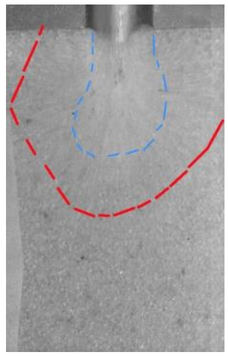

Figure 10. Projectile initially velocity 200 m/s. The red arc indicates compaction and blue arc indicates damage.

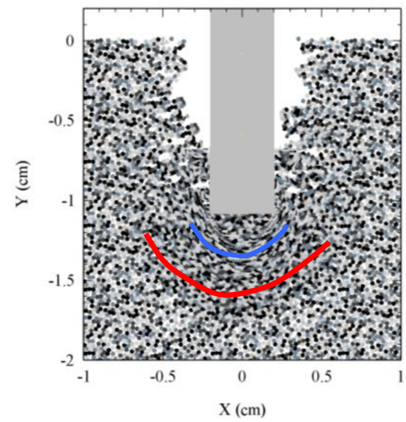

Figure 11. Mesoscale CTH simulation where the projectile is initially traveling 350 m/s. Much like experimental observations, simulation indicates regions of compaction (red) and damage (blue).

Figure 10 presents a simulation from the mesh-less peridynamics hydrocode formulation, EMU, in which a more physically realistic strain-to-fracture model has been utilized. Like CTH, EMU indicates a two-wave penetration event that propagates through the grain bed. Damage and fracture occur immediately ahead of the projectile as indicated in Fig. 10c, which is an enlargement of Fig 10b. This is similar to the experimentally results presented earlier.

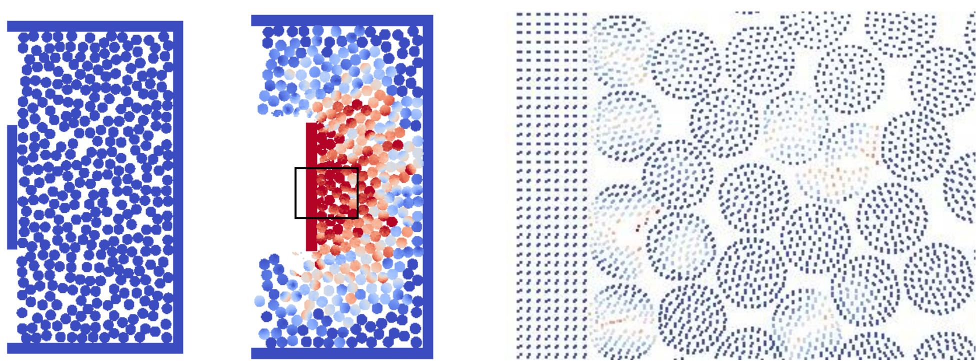

a) Initial Geometry b) 0.88 ms after impact c) Enlargement of square shown in b)

Figure 12. EMU simulation of projectile penetrating a) mono-dispersed granular media at 50 m/s. b) color indicates velocity c) Close up of b) where color indicates damage via a strain-to-failure fracture criteria.

3.2. Continuum Simulations

In addition to the mesoscale simulations, continuum simulations have been developed to capture the bulk compaction event. In order to construct the continuum equations of state we used the results from the mesoscale simulation. The compaction models of interest include the P-α and P-λ models. Figure 11 presents several results, where the dark lines are experimental obtained. Interestingly, the constitutive models built directly from the mesoscale simulations match the results from land mine data [Kerley Technical Services, report KTS05-3, Aug. 2005].

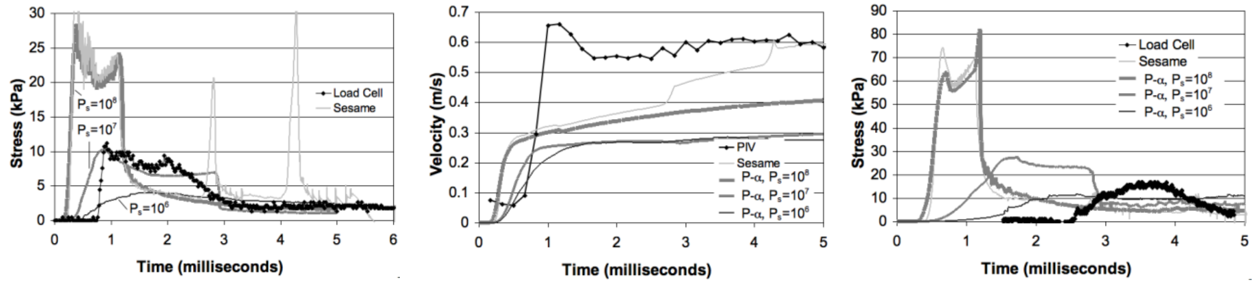

(a) Stress 4.58 cm from impact– Test 5 (b) Velocity 4.58 cm from impact –Test 5 (c) Stress 8.89 cm from impact– Test 8

Figure 13. Comparison of experimental data and numeric simulations of stress and velocity utilizing the sesame and Mie-Grüneisen equation of state with a P-α porous compaction model.

4. Discussion

We feel this work has made several contributions to our understanding of the dynamic compaction of granular materials: specifically, the formation of a compaction and damage wave and the compressive failure that occurs during the compaction and penetration event. The current work will continue into next academic year in order to completely document the progress to date. In addition to journal publications we will also be making presentations at conference proceedings.

5. References

[1] Liu, C. and Nagel, S. Sound in a grnular material: Disorder and nonlinearity. Physical Review B, 48(21), 1993.

[2] Brown, J. L. Vogler, T.J. Grady, D.E. Reinhart, W.D., Chhabildas, L.C and Thornhill, T. F. Dynamic Compaction of Sand, Shock Compression of Condensed Matter - 2007

DEPARTMENT OF DEFENSE

DEFENSE THREAT REDUCTION
AGENCY
8725 JOHN J. KINGMAN ROAD
STOP 6201
FORT BELVOIR, VA 22060
ATTN: A. LYALIKOV

DEFENSE TECHNICAL
INFORMATION CENTER
8725 JOHN J. KINGMAN ROAD,
SUITE 0944
FT. BELVOIR, VA 22060-6201
ATTN: DTIC/OCA

**DEPARTMENT OF DEFENSE
CONTRACTORS**

QUANTERION SOLUTIONS, INC.
1680 TEXAS STREET, SE
KIRTLAND AFB, NM 87117-5669
ATTN: DTRIAC